IEEE Photonics Journal
An IEEE Photonics Society Publication

Open Access

Frequency Quasi-Linear Swept Light Source Based on Multi-Frequency Time-Matched Spectrum Stitching

Volume 12, Number 6, December 2020

Lai Wen
Zhaoying Wang
Long Zhang
Quan Yuan
Chunfeng Ge
Tianxin Yang

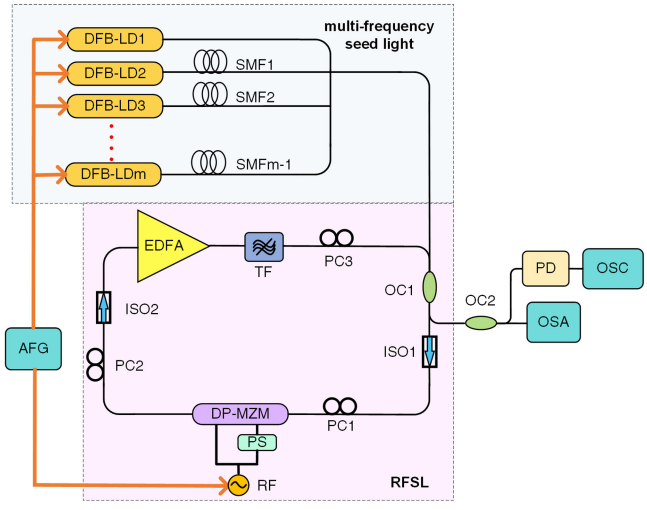

DOI: 10.1109/JPHOT.2020.3034916

Frequency Quasi-Linear Swept Light Source Based on Multi-Frequency Time-Matched Spectrum Stitching

Lai Wen, Zhaoying Wang, Long Zhang, Quan Yuan, Chunfeng Ge, and Tianxin Yang

Key Laboratory of the Ministry of Education on Optoelectronic Information Technology, School of Precision Instrument and Optoelectronics Engineering,Tianjin University, Tianjin 300072, China

DOI:10.1109/JPHOT.2020.3034916

Manuscript received September 29, 2020; revised October 24, 2020; accepted October 27, 2020. Date of publication October 30, 2020; date of current version November 19, 2020. This work was supported in part by the National Natural Science Foundation of China under Grants 61275084, 61605092 and in part by the Natural Science Foundation of Tianjin under Grant 18JCYBJC16800. Corresponding author: Zhaoying Wang (email: wangzy@tju.edu.cn).

Abstract: A novel frequency quasi-linear swept light source based on multi-frequency time-matched spectrum stitching and recirculating frequency shifter loop (RFSL) is proposed and successfully demonstrated. The seed light with different frequencies enters RFSL in turn through optical delay line to complete the frequency sweep and spectrum stitching of each band. Spectrum stitching can effectively reset the noise, suppress the accumulation of amplified spontaneous emission (ASE) noise and the spectral sideband noise in RFSL, and expand the sweep range several times without affecting the sweep linearity. A swept range of 5.227 nm is experimentally achieved with the noise range of 7.78 dB. Compared with the single-frequency sweep scheme that the noise variation is 9.03 dB, the sweep range is extended by more than three times. The Pearson's correlation coefficients (r) of the output swept signal is higher than -0.99996.

Index Terms: Frequency swept light source, stitching, RFSL, time-matched, noise reset, quasi-linear.

1. Introduction

Frequency swept light sources that establishes the mapping relationship between the frequency domain and the time domain through emitting different wavelengths at different times have been extensively used in the field of optical coherence tomography (OCT) [1], fiber sensor [2], lidar [3], absolute distance measurement [4], optical serial coherent analyzer (OSCAR) [5], multiple-frequency measurement [6], etc. All of these applications require the high resolution and low signal processing overhead, which can be fulfilled by a broadband swept laser source with low noise and high linearity in k-space.

The common methods of swept signal generation are divided into internal modulation and external modulation. In the internal modulation, mechanically tunable wavelength filters are inserted into the cavities of swept sources, such as Fabry-Perot tunable filters [7], tunable ratio optical couplers [8] and polygon mirror-scanning filters [9]. Therefore, the swept lasers can be linear only in wavelength over time rather than in frequency domain (k-space) due to the mechanical filtering

and the relationship of $k = 2\pi/\lambda$, even the nonlinearity caused by mechanical hysteresis is not considered. To solve this problem, several k-space swept systems have been proposed, such as Fourier domain mode locked (FDML) lasers [10], active mode locking (AML) fiber lasers [11], and monolithic integrated semiconductor laser diodes [12], *etc*. However, all of these methods have the inherent defect that the coherence of the light source deteriorates due to the internal modulation.

Different from internal modulation, external modulation is carried out outside the laser cavity and does not significantly change the coherence of the seed source, so it has been widely studied recently. The recirculating frequency shifter loop (RFSL) [13] is an effective external modulation scheme that guarantees the high linearity of the output signal in k-space, because the frequency of the light recirculating in the RFSL is shifted by a constant value (called swept step) in each circulation. However, the optical signal to noise ratio (OSNR) of the output decreases with the increase of the circulation number due to the accumulation of the amplified spontaneous emission (ASE) noise induced by the optical amplifier and the sideband noise induced by single-side-band (SSB) modulation of the seed light. Therefore, if a single frequency source is used as seed light, the output OSNR of RFSL deteriorates with the extension of swept range.

Some attempt has been studied to suppress the ASE noise by inserting additional optical switches in the RFSL such as the modulated semiconductor optical amplifier (SOA) [14]. However, the switch needs to be turned off for a long time (several microseconds) to achieve effective noise suppression, which is difficult to realize the stitching of swept pulses in time-domain. Meanwhile, the additional optical switch undoubtedly increases the complexity and the cost of the loop.

In our previous work, we proposed a parallel multi-wavelength swept light source [15] in which multiple seed lights were injecting into the RFSL at the same time and realized significant expansion of the sweeping bandwidth. In that method, the parallel injection of multi-channel seed light is beneficial to the signal light consuming more inversion particles, which alleviates the saturation of erbium-doped fiber amplifier (EDFA), to some extent, caused by ASE accumulation. But the output signals of different initial frequencies finish the swept at the same time, so it is necessary to demultiplex the signals to different photodetectors at the receiving end of the source system. This requires filters with steep edges and the transmission channel of the filters must be tuned synchronously with the sweep wavelength. While this type of filter is rare and is costly for practical applications.

In order to suppress the noise accumulation without increasing the difficulty of detection, we propose a "time-matched spectrum stitching" method in this paper. The multi-frequency seed light with equal frequency intervals is still used as in the parallel sweep scheme, but differently the frequencies pass through individual optical delay lines that produce different time delay before the RFSL. In this way, the frequency sweep of different frequency components is separated in the RFSL, i.e., when the seed light of the first frequency completes the frequency sweep within the frequency interval range, the seed light of the second frequency just finishes the time delay and enters the RFSL to start its frequency sweep. The accumulation of noise is suppressed because the noise will be reset due to the shutdown of the former frequency when the latter frequency starts to sweep. Besides, only one photodetector is needed at the receiving end, which greatly reduces the difficulty of the detection process and cuts the system cost.

We experimentally demonstrate that the stitching in both time domain and frequency domain are realized simultaneously and the swept signal outputs from a single port of 5.227 nm swept range is achieved within 7.78 dB noise variation, which is a significant improvement compare with single-frequency (the seed light has only a single frequency) sweep scheme. Besides, the spectrum stitching dose not affect the k-linearity of the swept output and the Pearson's correlation coefficients (r) is better than -0.99996.

2. Principles and Experimental Setup

The configuration of the swept light source is illustrated in Fig. 1 (optical fiber is marked by black lines and electric wire is marked by orange lines) and Fig. 2 qualitatively describes the signal of seed light and the swept light source.

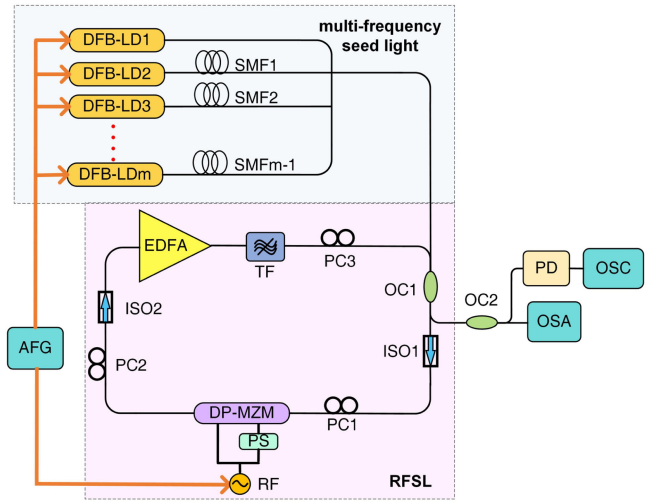

Fig. 1. Configuration of the swept light source. DFB-LDs, distributed feedback laser diodes. SMF, single mode fiber. OC, optical coupler. ISO, isolator. PC, polarization controller. DP-MZM, dual-parallel Mach-Zehnder modulator. PS, phase shifter. RF, radio frequency. EDFA, erbium-doped optical fiber amplifier. TF, tunable filter. PD, photodetector. OSC, oscilloscope. OSA, optical spectrum analyzer. AFG, arbitrary function generator.

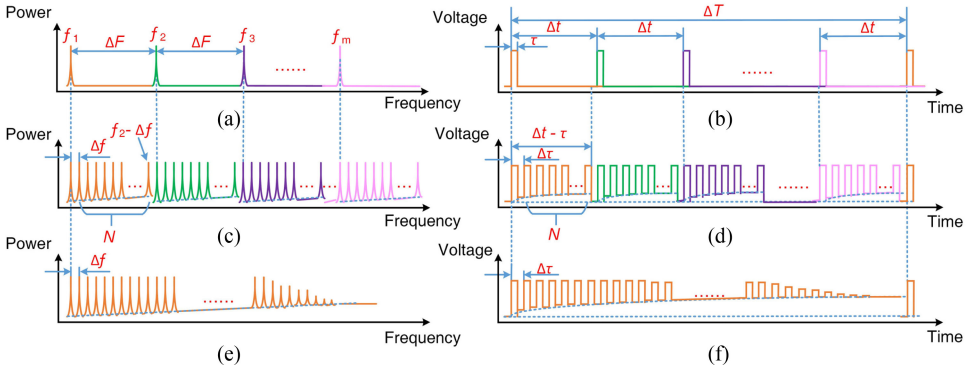

Fig. 2. The output of multi-frequency seed light and the swept light source in frequency-domain and time-domain. (a) The initial frequencies of seed lights. f_m is the initial frequency of the mth seed light. ΔF is the frequency spacing between the adjacent seed lights. (b) The initial seed pulses. τ is the width of seed pulse. ΔT is the period of seed pulse sequence. Δt is the delay time induced by the SMFs. (c) The swept spectrum of multi-frequency seed light. Δf is the swept step. N is the circulation number in RFSL of each seed light. (d) The output swept pulse sequence of multi-frequency seed light. $\Delta\tau$ is the round-trip time in RFSL. (e) The swept spectrum of single-frequency seed light. (f) The output swept pulse sequence of single-frequency seed light.

As shown in Fig. 1, the outputs of m distributed feedback laser diodes (DFB-LDs) are used as multi-frequency seed light. The frequencies of DFBs outputs are f_1, f_2, …, f_m, and the frequency interval is ΔF, as shown in Fig. 2(a). They are modulated by an arbitrary function generator (AFG) into pulses with pulse width (τ) and pulse period (ΔT) respectively, as shown in Fig. 2(b). Single mode fibers (SMFs) of different lengths are connected to the DFB-LDs to introduce a fixed delay time, denoted as Δt, between adjacent frequencies before they are injected into RFSL.

The RFSL consists of an optical coupler (OC), two isolators (ISO), three polarization controllers (PC), an erbium-doped optical fiber amplifier (EDFA), a tunable filter (TF), and a dual-parallel Mach-Zehnder modulator (DP-MZM). The DP-MZM in single-side-band (SSB) modulation state works as a frequency shifter [16]. The product of round-trip time of the optical loop and the expected sweep pulse number is exactly equal to the delay time in the SMF. The swept step (Δf) of the RFSL is

determined by the RF signal frequency applied on the DP-MZM, and the frequency interval is the product of swept step and the expected sweep pulse number. The on-off of the RF signal is also controlled by the AFG. Obviously, the frequency shift of the seed light will be stopped when the RF signal is turned off, so controlling the on/ off of the RF signal at the right time is one of the key steps to achieve spectrum stitching. In our multi-frequency stitching scheme, the switching period of the RF signal is equal to the delay time, and the turn-on time lasts until the falling edge of the last sweep pulse of each initial frequency. This setup ensures that each seed light will start to sweep just after the time delay and will be turned off exactly after its last frequency shifted in RFSL. The schematic diagrams of swept spectrum and waveform of multi-frequency seed light are shown in Fig. 2(c) and (d) respectively. When the sweep starts, half power of the first frequency output directly as the start frequency of the swept output. The other half is sent into the RFSL and it is shifted N times with enabled RF signal. During this process, ASE noise induced by the EDFA and sideband noise induced by single-side-band modulation of the seed light will be accumulated as the number of circulation increases. Then the RF signal is turned off in the subsequent time until the rising edge of the next pulse. The accumulated noise is reset at the same time. When the RF signal is turned on again, the second frequency just passes through the delay SMF and starts the same sweeping as the first frequency. As shown in Fig. 2(c) and (d), every time a new frequency of seed light is injected into the RFSL, the noise is reset back to the initial value. The sweep process is repeated for each frequency of the multi-frequency seed light. So far the sweep light source completes the stitching in one period.

For analyzing the ASE noise accumulation during the sweep process, the RFSL can be simplified as a number of cascade EDFAs [17]. The accumulated noise ΣP_{ASE} of the light source can be expressed as the sum of the noise introduced by each amplifier after amplification and attenuation in the subsequent optical path:

$$\sum P_{ASE} = P_{ASE1} L_2 G_2 L_3 G_3 \ldots L_N G_N + P_{ASE2} L_3 G_3 \ldots L_N G_N + \ldots + P_{ASEN}, \tag{1}$$

where N is the number of EDFAs, G_i and P_{ASEi} are the gain and noise power of the ith ($i = 1, 2, 3, \ldots, N$) EDFA respectively, L_i is the loop loss of the ith circulation and includes modulation loss and insertion loss. For every single EDFA, the noise is:

$$P_{ASEi} = F_i G_i B_i h\upsilon \quad (i = 1, 2, 3, \ldots \quad, N), \tag{2}$$

where F_i is the noise coefficient, $h\upsilon$ is the photon energy and B is the bandwidth of the TF.

In the corresponding mathematical model of RFSL, the noise coefficients of the EDFAs are the same and the filter bandwidth also remains unchanged, there is:

$$\sum P_{ASE} = FBh\upsilon \left(G_1 L_2 G_2 L_3 G_3 \ldots L_N G_N + G_2 L_3 G_3 \ldots L_N G_N + \ldots + G_N\right). \tag{3}$$

Ideally, the gain of EDFA can just compensate the loss in the loop and the gains of the EDFAs of different frequencies are identical, then:

$$L_i G_i = 1 \text{ and } G_1 = G_2 = \ldots = G_N = G. \tag{4}$$

So Eq. (3) can be rewritten as:

$$\sum P_{ASE} = NFBh\upsilon G. \tag{5}$$

Therefore, the accumulated noise in Eq. (5) shows the noise power when f_1 finishes N cycles sweep. It can be concluded from Eq. (5) that the trend of noise accumulation is approximately a linear function with the increase of the circulations number in the ideal case. Correspondingly, the continuous accumulation of noise also leads to the increase of bottom noise of sweep pulse in time-domain waveform as shown in Fig. 2(c) and (d). However, according to the multi-frequency seed light sweeping process described above, the noise power of the whole sweep process will also not exceed this value due to the effect of noise reset. Of course, in practice, since the EDFA amplifies all the input light including signal and noise, the signal gain will gradually decrease with the increase of noise.

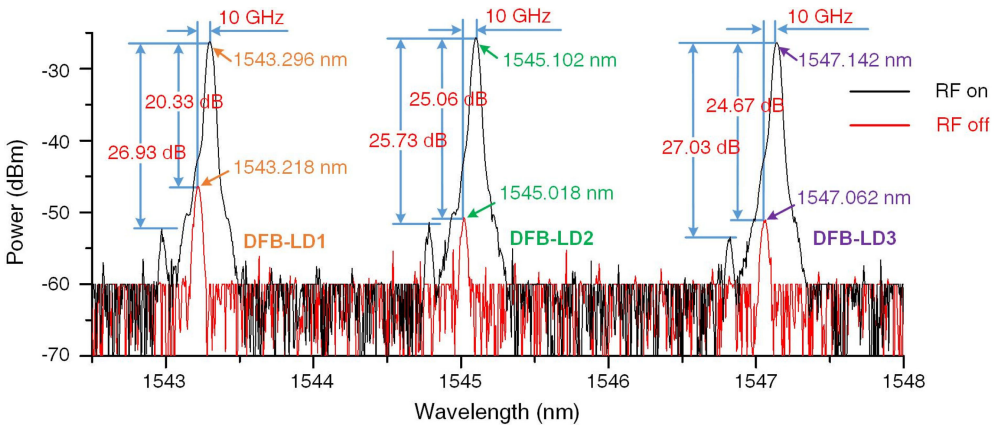

Fig. 3. The output spectrum of the three DFB-LDs after being simultaneously shifted only once by the DP-MZM without pulse modulation and time delay.

For comparison, we replace the multi-frequency seed light in Fig. 1 with the single-frequency seed light and schematic diagram of the swept output are shown in Fig. 2(e) and (f). In the single-frequency sweep scheme, the input frequency sweeps continuously with a step of Δf without interruption and stitching. To obtain the same swept range as that in the multi-frequency seed light, the expected circulation number is $m(N+1)-1$ (m is the frequency number of multi-frequency seed light). Therefore, the noise power of single-frequency sweep scheme is described as:

$$\sum P_{ASE(sf)} = (mN + m - 1)\, FBhvG \tag{6}$$

Since the noise accumulates without any reset, the EDFA is gradually saturated by the accumulated noise and the signal amplification is insufficient to compensate for the loop loss. As a result, the power of the signal decreases and is finally submerged into the noise, as shown in Fig. 2(e) and Fig. 2(f). The comparison between the two sweep schemes proves that the stitching scheme optimizes the OSNR of RFSL to some extent.

3. Experimental Results

A swept light source was built with the configuration shown in Fig. 1. In theory, any swept step can be obtained by changing the frequency of the RF signal, and in the following experiments, the swept step is set to 10 GHz (0.08 nm@1550 nm wavelength) for showing a clear spectrogram since the resolution of the OSA (Ando, AQ6315A) is 0.05 nm. Three DFB-LDs with ~500 kHz linewidth are used. The output frequencies of DFB-LDs are controlled by integrated temperature control chip. The regulation precision is 0.01 °C, corresponding to 0.01 nm wavelength precision theoretically.

Fig. 3 shows the output spectrum of the three DFB-LDs after being shifted only once by the DP-MZM without pulse modulation and time delay. The black line and the red line are the spectrum when the driven RF signal is on or off respectively. As can be observed, the three frequency components modulated by the DP-MZM are all shifted by 10 GHz in the frequency domain. The optical signal is strongly attenuated in the RFSL when the RF signal is off and the optical power difference is more than 20.33 dB, which means that the DP-MZM can work as a switch of the optical loop. The side mode suppression ratio (SMR) of each frequency component is larger than 25.73 dB when the RF signal is on. It proves that other sideband generated by the modulation can be considered as noise. Obviously, it is also amplified and accumulates together with ASE noise in the sweeping process.

The spectrum and the waveform of both the seed lights and the swept output are illustrated in Fig. 4. Temperature control chip makes that the output wavelengths of the three DFB-LDs are 1543.105 nm (λ_1), 1544.870 nm (λ_2) and 1546.639 nm (λ_3), corresponding the frequency

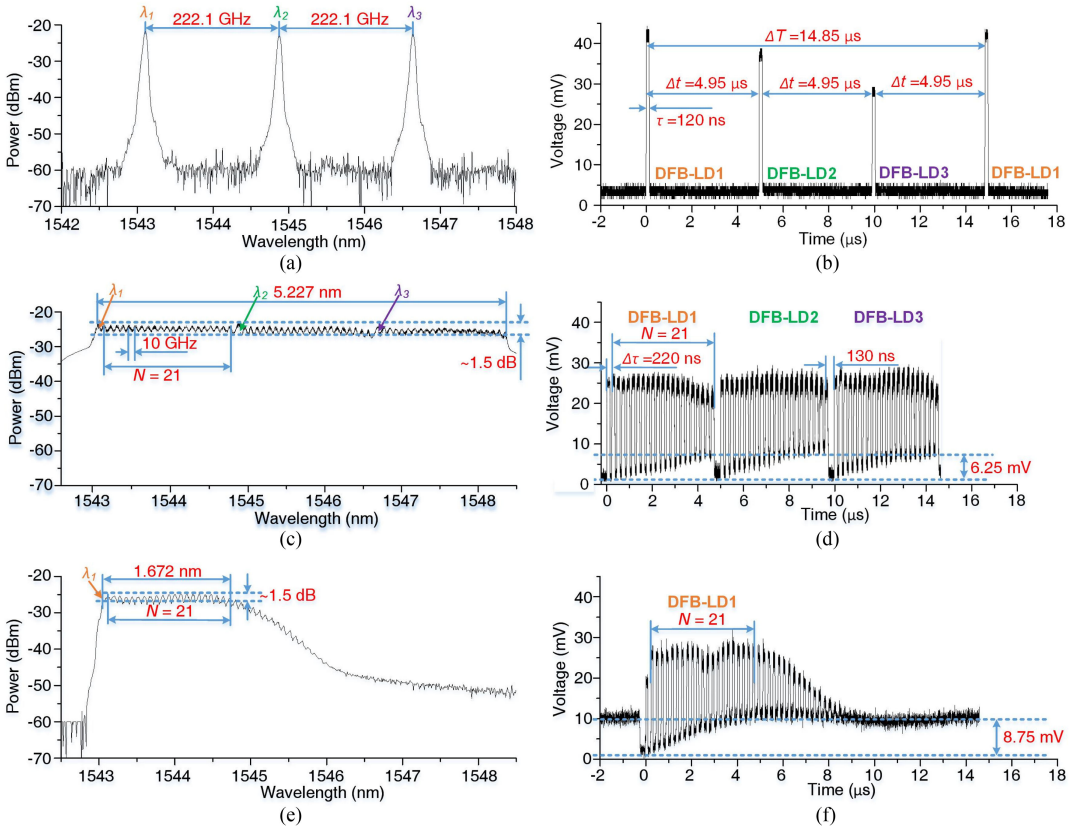

Fig. 4. The experimental results in the frequency-domain and in the time-domain. (a) The spectrum of the multi-frequency seed lights. λ_m is the initial wavelength of the *m*th DFB-LD. (b) The waveform of the pulse modulated seed lights. τ is the width of seed optical pulse; ΔT is the period of seed optical pulse sequence; Δt is the delay time of the SMF. (c) The output swept spectrum of the multi-frequency seed lights. *N* is the number of circulation of each initial frequency components. (d) The swept output waveform of multi-frequency seed light in one swept period. $\Delta\tau$ is the round-trip time of the RFSL. (e) The output swept spectrum of the single-frequency seed light. (f) The swept output waveform of single-frequency seed light in one swept period.

are 194.4132 THz, 194.1911 THz and 193.9690 THz. The frequency spacing between them is 222.1 GHz. In this way, when we sweep the frequency in step of 10 GHz, the number of cycles can be approximated as an integer, that is N = 21. The values of the wavelength shown in Fig. 4(a) are detected by a wavelength-meter (EXFO, WA-1100, the resolution is 0.001 nm) for a higher accuracy than the OSA. The pulse waveform obtained in the time domain is sent to the PD (LSIPD-0.1S, response time 0.25 ns) and the oscilloscope for detection. The three DFB-LDs are synchronously modulated into pulses with the pulse period of 14.85 μs and the pulse width of 120 ns as shown in Fig. 4(b).

Fig. 4(c) shows the output swept spectrum of the multi-frequency stitching scheme. The stitching spectrum covers a range of 5.227 nm and the flatness of the swept spectrum is $\pm$0.765 dB. The round-trip time of the RFSL ($\Delta\tau$) is about 220 ns according to Fig. 4(d) and the period of RF signal is set to 4.95 μs, which is equal to the delay time between two adjacent DFB-LDs induced by the SMFs. A gap of 130 ns time between adjacent DFB-LD signals is set in Fig. 4(d) for clearly distinguishing the swept range of each DFB-LD. The gaps can be changed or removed by adjusting the length of the SMFs slightly. It is clear from Fig. 4(d) that the accumulated noise is reset at the stitching point. The noise baseline of 66 flat output pulses increases from 1.25 mV to 7.5 mV, (increased by 6.25 mV, marked by blue dotted line), corresponding to 7.78 dB noise variation.

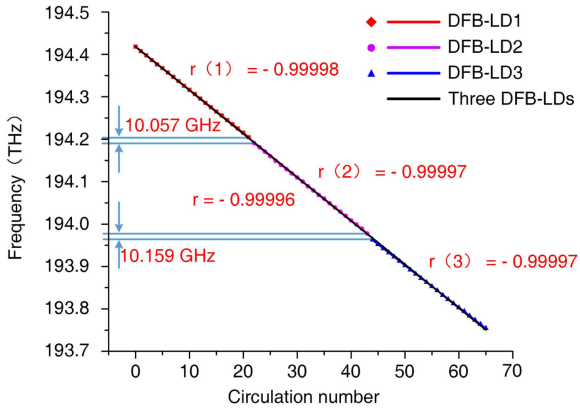

Fig. 5. The linearity of swept output in frequency domain.

In order to observe and analyze the phenomenon of noise accumulation, DFB-LD2 and DFB-LD3 were turned off and only DFB-LD1 was kept running for comparison. As shown in Fig. 4(e), the spectrum power gradually decreases with the sweep process and the signal intensity is fading (power drop $>$1.5 dB) after 1.672 nm. The power of the pulse sequence in time-domain also declines and the pulse is finally submerged into the noise as shown in Fig. 4(f). The degradation of the spectrum and the waveform confirms that the signal has not enough gain to compensate the loss in the RFSL. The bottom noise increases from 1.25 mV to 10 mV, (increased by 8.75 mV, marked by blue dotted line) in the waveform and the corresponding variation range of the optical noise is 9.03 dB, which is 1.25 dB higher than that in Fig. 4(d).

The linearity of sweep output in frequency domain is shown in Fig. 5. The Pearson's correlation coefficients (r) of the three sweep spectrum are -0.99998, -0.99997 and -0.99997 respectively. The tiny frequency error is mainly from the phase noise of the RF signal, which is -75 dBc/Hz@10 GHz in our experiments. The linearity of the stitching spectrum is -0.99996. The frequency spacing between the 22nd swept output signal of DFB-LD1 and the initial output of DFB-LD2 is 10.057 GHz and the frequency spacing between the 22nd swept output signal of DFB-LD2 and the initial output of DFB-LD3 is 10.159 GHz, which deviate from the theoretical value of 10.000 GHz by 0.57% and 1.59%. The stitching-error is mainly caused by the thermal drift of the initial seed frequency. This can be decreased with a more accurate temperature control of DFB-LDs.

4. Conclusion

In conclusion, we proposed and demonstrated a frequency quasi-linear swept light source by using a recirculating frequency shifter loop (RFSL). This is based on a multi-frequency time-matched spectrum stitching technique. With three DFB-LDs as seed sources, a swept spectrum of 5.227 nm with 7.78 dB variation of noise and >-0.99996 swept linearity in k-space is achieved. The variation range of noise decreases by 1.25 dB and the swept range is broaden more than three times compare with single-frequency scheme. The stitching method solves the problem of difficult detection and application in parallel multi-wavelength frequency swept systems effectively. Besides, the swept range can be further broadened by adjusting the sweep range of each frequency component or increasing the number of stitched frequencies.

References

[1] D. Huang, F. Li, C. Shang, Z. Cheng, and P. K. A. Wai, "Reconfigurable time-stretched swept laser source with up to 100 MHz sweep rate, 100 nm bandwidth, and 100 mm OCT imaging range," *Photon. Res.*, vol. 8, no. 8, pp. 1360–1367, Aug. 2020.

[2] Q. Yuan *et al.*, "A fast linearly wavelength step-swept light source based on recirculating frequency shifter and its application to FBG sensor interrogation," *Sensors*, vol. 19, Jan. 2019. Art. no. 593.
[3] Z. lu *et al.*, "Broadband linearly chirped light source with narrow linewidth based on external modulation," *Opt. Lett.*, vol. 43, no. 17, pp. 4144–4147, Sep. 2018.
[4] X. Wu, H. Wei, H. Zhang, L. Ren, Y. Li, and J. Zhang, "Absolute distance measurement using frequency-sweeping heterodyne interferometer calibrated by an optical frequency comb," *Appl. Opt.*, vol. 52, no. 10, pp. 2042–2048, Apr. 2013.
[5] R. Li *et al.*, "Optical serial coherent analyzer of radio-frequency (OSCAR)," *Opt. Express*, vol. 22, no. 11, pp. 13579–13585, Jun. 2014.
[6] R. Li, H. Chen, Y. Yu, M. Chen, S. Yang, and S. Xie, "Multiple-frequency measurement based on serial photonic channelization using optical wavelength scanning," *Opt. Lett.*, vol. 38, no. 22, pp. 4781–4784, Dec. 2013.
[7] M. Chen, W. Jia, J. He, X. Qin, and G. Zheng, "Development of swept source based on dual filtering," *Opt. Precis. Eng.*, vol. 26, no. 10, pp. 2355–2362, Oct. 2018.
[8] G. Lin, J. Chang, Y. Liao, and H. Lu, "L-band Erbium-doped fiber laser with coupling-ratio controlled wavelength tunability," *Opt. Express*, vol. 14, no. 21, pp. 9743–9749, Oct. 2006.
[9] S. M. R. Motaghian Nezam, "High-speed polygon-scanner-based wavelength-swept laser source in the telescope-less configurations with application in optical coherence tomography," *Opt. Express*, vol. 33, no. 15, pp. 1741–1743, Aug. 2008.
[10] J. P. Kolb, T. Pfeiffer, M. Eibl, H. Hakert, and R. Huber, "High-resolution retinal swept source optical coherence tomography with an ultra-wideband Fourier-domain mode-locked laser at MHz A-scan rates," *Biomed. Opt. Express*, vol. 9, no. 1, pp. 120–130, Jan. 2018.
[11] H. D. Lee, Z. Chen, M. Y. Jeong, and C. Kim, "Simultaneous dual-band wavelength-swept fiber laser based on active mode locking," *IEEE Photon. Technol. Lett.*, vol. 26, no. 2, pp. 190–193, Jan. 2014.
[12] T. DiLazaro and G. Nehmetallah, "Large-volume, low-cost, high-precision FMCW tomography using stitched DFBs," *Opt. Express*, vol. 26, no. 3, pp. 2891–2904, Feb. 2018.
[13] K. Shimizu, T. Horiguchi, and Y. Koyamada, "Frequency translation of light waves by propagation around an optical ring circuit containing a frequency shifter: I. Experiment," *Appl. Opt.*, vol. 32, no. 33, pp. 6718–6726, Nov. 1993.
[14] M. Wan *et al.*, "Rapid, k-space linear wavelength scanning laser source based on recirculating frequency shifter," *Opt. Express*, vol. 24, no. 24, pp. 27614–27621, Dec. 2016.
[15] Q. Yuan, Z. Wang, L. Song, C. Ge, Z. Lu, and T. Yang, "Ultrafast wavenumber linear-step-swept source based on synchronous lightwave synthesized frequency sweeper," *IEEE Photon. J.*, vol. 11, no. 1, Feb. 2019, Art. no. 1400108.
[16] Z. Jiang, Z. Wang, T. Xie, Q. Yuan, and C. Ge, "Dual-frequency light source with widely tunable frequency difference based on single-side-band modulator," *Opt. Commun.*, vol. 445, pp. 50–55, Aug. 2019.
[17] H. Mo, "Study on noise characteristics of cascade erbium-doped fiber amplifier," *Comput. Sci. Technol.*, vol. 4, no. 6, pp. 1517–1518, Nov. 2008.